A METHOD FOR PREDICTING CT-LIN CONTACT USING CANDU 6 INSPECTION RESULTS

Bill Rankin – NB Power Nuclear, Point Lepreau Generating Station
Paul J. Sedran – Canadian Power Utility Services (CPUS) Limited

ABSTRACT

In the Point Lepreau Generating Station (PLGS), the Liquid Injection Nozzle (LIN) was installed 120 mm below the Calandria Tube (CT) above it. Since the creep sag rate of the fuel channel exceeds that of the LIN, CT-LIN contact may be possible. CT-LIN contact is considered unacceptable since it will result in fretting damage to the CT.

Because of concerns about potential CT-LIN contact, various measurements of CT-LIN gap and CT and LIN elevations have been performed in different CANDU 6 reactors.

A method for predicting time-to-contact of the CT with the LIN, using inspection data, was developed by CPUS for PLGS in 2005. The method involves using updated CDEPTH fuel channel models to predict CT creep sag rates and using LIN creep sag rates derived from CT-LIN gap measurements. CT-LIN time-to-contact predictions using this method indicated no contact before 200 kEFPH, resulting in the decision to cancel further CT-LIN inspections in PLGS. The same assessment was undertaken for Gentilly-2 (G-2) but is awaiting further inspection results.

For CANDU 6 reactors without CT-LIN gap measurements, it is proposed that the LIN initial sag and sag rate deduced from measurements in Wolsong 1 and Wolsong 4 can be used to model the sag behaviour of the LIN.

CT-LIN contact predictions can then be performed for any CANDU 6 reactor using:

1. Updated CDEPTH models to predict CT sag versus time in-service
2. Sag measurements from Wolsong Units 1 and 4 to determine LIN sag versus time in-service, or if available, CT-LIN gap measurements.

The development of the above method is outlined in this paper. Examples of CT-LIN time-to-contact predictions are presented for PLGS and G-2.

Nomenclature

Elevation - vertical distance, measured as positive in the downward direction from the horizontal reference plane. Each fuel channel has its own horizontal reference plane which contains the centerline of the un-deformed Pressure Tube (PT).

Q21-L5 – the point on the bottom of the CT of Q21 that would contact the top of LIN 5
L5-Q21 – the point on the top of the LIN that would contact with Q21-L5

1. Introduction

In the Point Lepreau Generating Station (PLGS), the Liquid Injection Nozzle (LIN) was installed with a 120 mm gap relative to the Calandria Tube (CT) above it. Since the creep sag rate of the fuel channel exceeds that of the LIN, CT-LIN contact was possible.

CT-LIN contact is considered unacceptable since it would have resulted in fretting damage to the CT. Fuel channel creep sag, leading to CT-LIN contact is therefore considered to be a life-limiting factor for CANDU fuel channels. Various analyses related to CT-LIN contact for PLGS and G-2, performed in 2005 - 2007, have led to the development of a general method for predicting CT-LIN contact times, presented in this paper. The following provides a summary of the historical background for this paper.

In response to the CT-LIN contact issue for the CANDU 6, ultrasonic measurements of CT and LIN sag were performed in Wolsong Units 1 and 4 in 2000. Optical CT-LIN gap measurements were performed in G-2 in 2003 and 2006 and in 2004 in PLGS. The optical CT-LIN gap measurements were supplemented by Pressure Tube (PT) sag measurements for specific PTs. These inspections were designed to allow for the measurement of the in-service elevations at discrete points along the LIN, which were previously unknown.

In 2005, the 2004 CT-LIN gap measurement data for PLGS were used with standard CDEPTH fuel channel models to predict CT-LIN contact times. For each fuel channel, linear equations were used to represent the elevations the contact points at the bottom of the CT and at the top of the LIN versus time in-service. Contact was predicted by solving for the time at which the two elevations would be equal. It was predicted that CT-LIN contact could first occur at 188 kEFPH, which was unacceptable [1]. However, considerable conservatism was found in the standard fuel channel models.

In 2005, in response to the unacceptable time-to-contact predictions, a reassessment [2] of CT-LIN time-to-contact was performed for critical fuel channels in PLGS which involved:

1. the development and use of an updated CDEPTH fuel channel model to predict fuel channel sag
2. the use of inspection data to define an in-service elastic curve[1] for the LIN that was intended to be used to predict LIN creep sag rates.

It was predicted in References [2] and [3] that CT-LIN contact in PLGS would occur well after reactor shutdown at 185 kEFPH for refurbishment. On the basis of that assessment, no further work related to CT-LIN contact was performed for PLGS.

The same analysis was performed [4] for G-2, using data from the 2003 and 2006 inspections. Unfortunately, anomalies in the measurements prevented the use of the G-2 CT-LIN gap data in the same way that the PLGS data was used. Further inspections are planned for G-2

For the PLGS and G-2 assessments, it was expected that LIN creep sag rates would be obtained from the various inspection measurements, but this was not achieved. In the absence of empirical LIN creep sag rates for PLGS, two creep sag rate cases were used: (1) assuming no future sag of the LIN and (2) assuming a first-principles estimated sag rate, which was a less-than-satisfactory approach.

Note 1 – operating sag displacement curve from elastic sag deflections under dead weight loading plus creep sag deformation due to irradiation and thermal creep

At this point, the ultrasonic measurements of LIN sag performed by KEPRI in Wolsong Units 1 and 4 [5] proved to be invaluable. From those measurements, the initial sag and the rate of LIN creep sag were deduced. It is proposed that the initial sag and creep sag rate of the Wolsong LIN be used to predict the sag behaviour of the LIN for other CANDU 6 reactors.

In view of the PLGS and G-2 assessments and the Wolsong inspection data, the following general method is proposed for predicting CT-LIN contact for a given CANDU 6 fuel channel when no inspection results are available:

1. Use the updated fuel channel model to predict CT sag versus time in-service and set up a linear equation for the CT contact point elevation versus time in-service
2. Use the Wolsong LIN initial elastic curve and creep sag rates and set up an equation for the LIN contact point elevation versus time in-service.
3. Solve the system of equations to predict the time-to-contact

When reliable CT-LIN gap measurements are available, a reactor-specific equation for LIN elevation can be derived using the CT-LIN gap measurements.

Examples of CT-LIN time-to-contact predictions using this method are presented in this paper for PLGS and G-2.

To validate the proposed CT creep sag prediction method, CT creep sag rates were predicted for the Row Q CTs in G-2 using an alternative method and were compared with those of the proposed method.

In the CANDU 6 reactor CT-LIN contact will first occur between the Row Q channels and LIN #5. Analysis results are presented only for the Row Q fuel channels in this paper.

2.0 Input Data Used in the Assessment

This section provides an outline of the input data that was used to develop the proposed method.

2.1 PT Sag Measurements

PT sag measurements in PLGS, presented in Figure 1, were performed during fuel channel inspections in 1986, 1988, 1991, 1998, 1999, and 2004.

The sag measurements were used in the development of updated CDEPTH fuel channel models.

2.2 PT In-Service Dimensions

An example of diametral expansion and wall thinning with time in-service for the PLGS PTs is presented in Figure 2 for F06, which was inspected at 157 kEFPH.

In the standard CDEPTH fuel channel model, uniform design-basis PT dimensions are assumed. For F06, an incremental increase in PT stiffness would result from the observed deformation of the PT. These dimensional changes suggested that PT dimensions should be investigated as possible parameters to be updated in the CDEPTH fuel channel models

2.3 CT In-Service Dimensions

In the course of this work it was found that the stiffness of F06 at 157 kEFPH is significantly higher than that predicted with the standard CDEPTH model, which led to the hypothesis that CT ovalisation at the spacers might have stiffened the CT of F06.

For F06, CT inner diameter values at 72 angular locations were obtained along the length of the CT using data from the 2004 inspection of PLGS. Figure 3 presents a plot of CT maximum inner radius versus axial position for F06.

Figure 1 – Measured PT Sag versus EFPH for the PLGS PTs

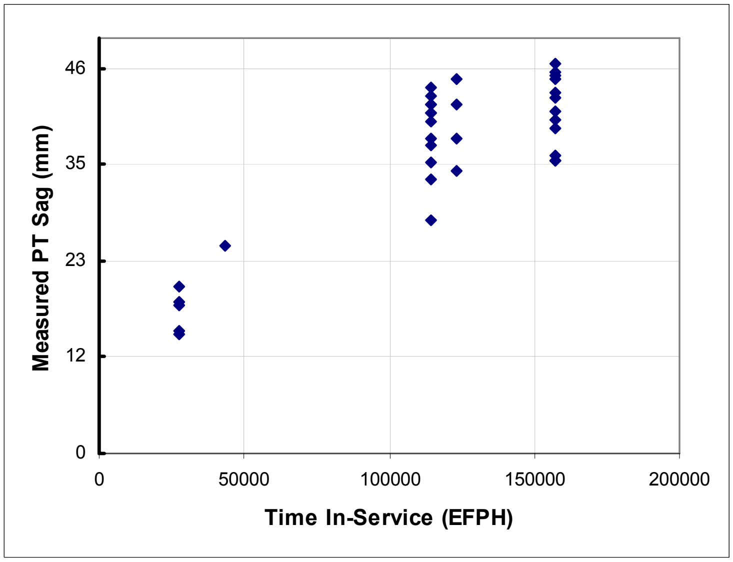

Although the CT-PT gap data used in Figure 3 appears reasonable, the inspection teams could not verify the accuracy of the data. The work proceeded keeping in mind that the CT-PT gaps required verification.

Figure 2 – In-Service PT Dimensions for F06 in PLGS

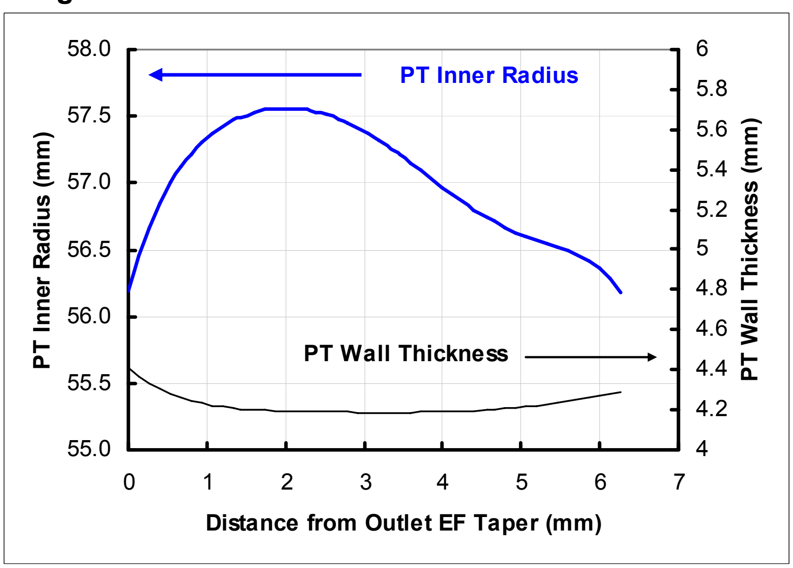

2.4 PT- CT Gap Measurements at 157,000 EFPH

PT-CT gap measurements from the 2004 fuel channel inspection were provided in Reference [6]. As an example, Figure 4 presents the gap data for F06 at 157 kEFPH. The data for specific channels was used to find the PT-CT gaps at L5-Q07 and L5-Q08.

Figure 3 – CT Maximum Inner Radius vs Axial Position for F06 Based on Preliminary CT- PT Gap Measurements

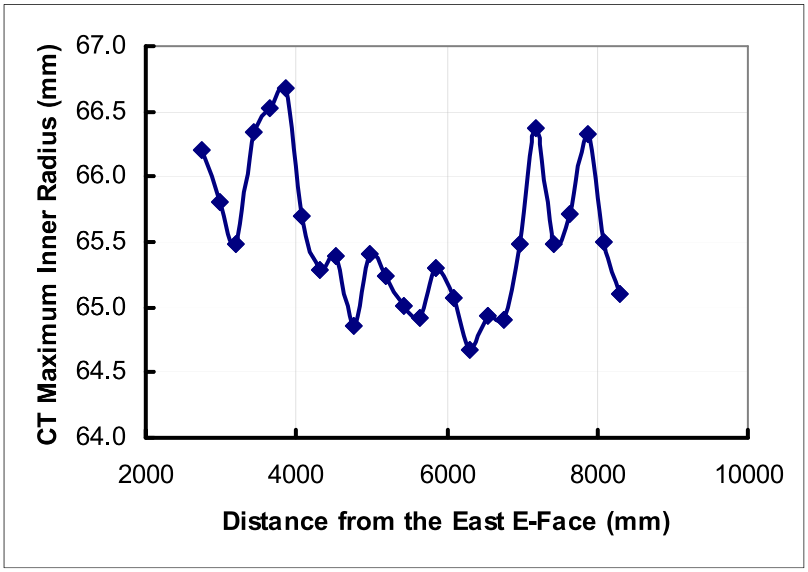

CT inner diameter at each axial position was measured as varying with angular position. The figure presents the maximum inner radius measured at each axial location.

Figure 4 – CT-PT Gap Measurements for F06 at 157 kEFPH

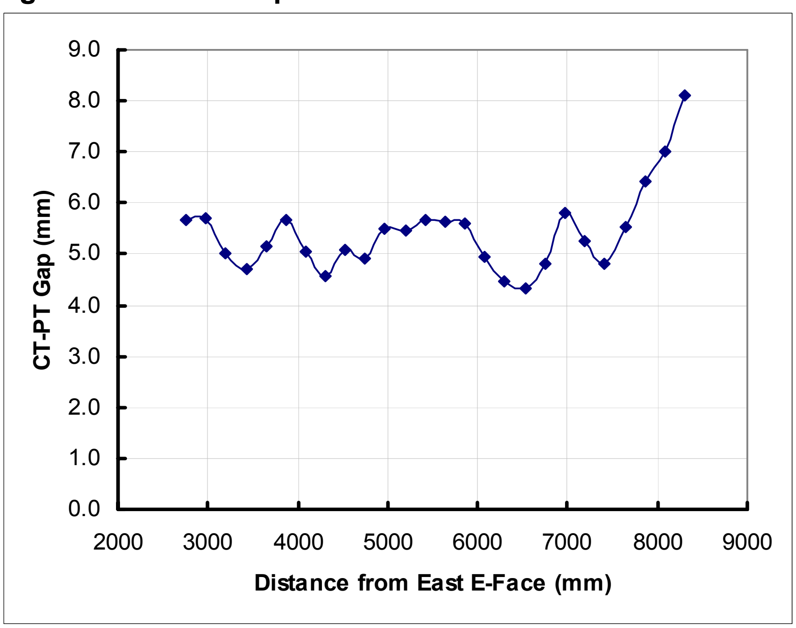

2.5 CT-LIN Optical Gap Measurements

Table 1 presents the 2004 optical gap measurement data [7] for the Row Q channels in PLGS. Note that the channels were fuelled during the gap measurements.

Table 1 – Optical Measurements of CT- LIN Gaps For Row Q in the 2004 Inspection

Fuel Channel	LIN	CT-LIN Gap (mm)
Q06	#5	10.1
Q07	#5	13.8
Q08	#5	14.2
Q09	#5	15.0

2.6 CT Spring-Back Measurements

During the 2004 inspection of the PLGS fuel channels, the following measurements were taken:

- with the channel fuelled (all 12 fuel bundles installed) the CT-LIN gap at F06-L2 was measured to be 16.2 mm
- with the channel defuelled the CT-LIN gap at F06-L2 was measured to be 20.7 mm

Therefore, the nominal elastic spring back deflection of the CT at F06-L2 was 4.5 mm.

2.7 LIN In-Service Sag Measurements from Wolsong 1 and 4

Reference 5 gives the ultrasonic inspections that were performed in Wolsong Units 1 and 4. The measurements in Table 2 proved to be very useful for determining the initial elastic curve and in-service elastic curve for the LIN.

Table 2 – Wolsong LIN Sag Measurements

Reactor	Inspection EFPH	LIN Sag (mm)
Wolsong 1	4512	4.9
Wolsong 4	126744	8.3

The LIN sag was measured with an ultrasonic probe in View Port #2. It was assumed that the probe was centred in the view port, 1.243 m from the pinned end of the LIN.

2.8 LIN Installation Data

LIN installation measurements and fuel channel dimensions were used to calculate the elevation of the support points of the LIN, presented in Table 3, which are required for the LIN elastic curve. Note that elevations for all points on the LIN are always relative to the horizontal datum through the centreline of the fuel channel.

Table 3 – Elevation of the PLGS LIN Support Points

LIN	Elevation (mm)
#5	120.24

2.9 Reactor Operating History

Until 1997, PLGS operated with a daily average power rating close to 100% (not including zero-power days). Starting at about 100 kEFPH, the reactor underwent gradual power derating. Figure 5 is a plot of lifetime daily averaged reactor power at various times in the operating history of PLGS. The specific EFPH values at which the daily lifetime averaged reactor power levels were calculated are listed on the figure.

The power derating of PLGS, seen in Figure 5, moderated PT flux and temperature conditions compared to design-basis PT operating conditions.

In the standard CDEPTH fuel channel models for PLGS, PT fast neutron flux values were assumed to be constant with time and were based on data compiled in 1993 when the average lifetime power for PLGS was 98.3 % Reactor Power. From Figure 5, a lifetime average daily power of 98.3 % would be applicable to PLGS up to 100 kEFPH but not later. Therefore, the fast neutron flux profiles in the standard CDEPTH models overestimate the actual fluxes experienced by the PLGS fuel channels after 100 kEFPH of operation.

Figure 5 – Lifetime Averaged Reactor Powers Computed at EFPH Values for the Various Inspections of PLGS

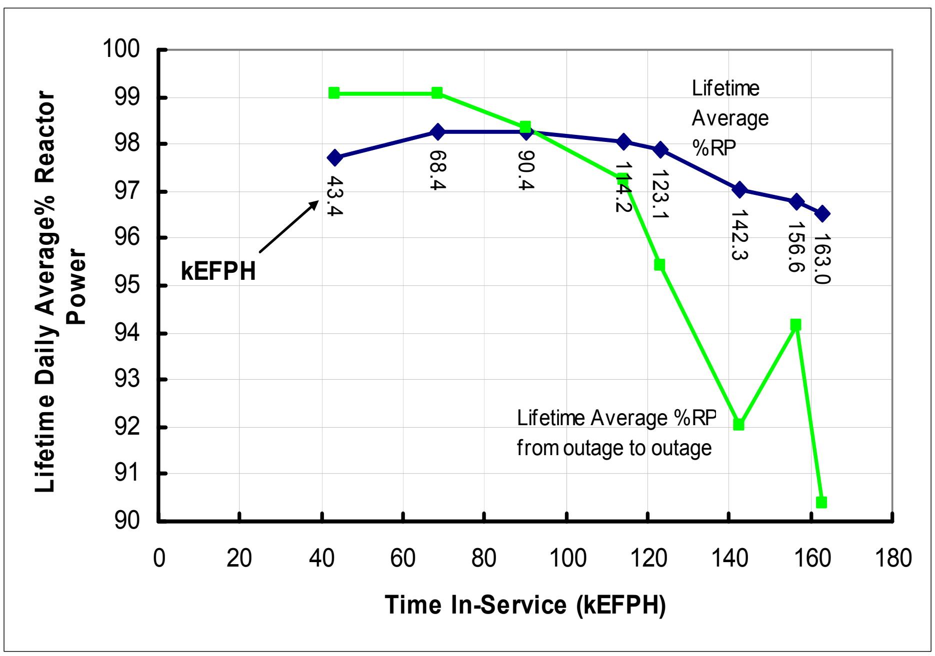

Each of the kEFPH values given represent times at which the reactor was shut down for inspections or SLAR outages.

3.0 Analytical Methods

3.1 CDEPTH 8.2

CDEPTH 8.2 is the code that was used to predict fuel channel sag deformation with time in-service for this paper. The equivalence of CDEPTH 8.2 and CDEPTH 9.0 for fuel channel sag predictions was documented in Reference [1].

3.2 ANSYS 9.0

ANSYS 9.0 was used to predict the initial elastic curve of the LIN.

3.3 Time-to-Contact Predictions

Time-to-contact predictions were generated for each potential contact point on LIN #2 and LIN #5 with the CTs in Row F and Q, respectively. The time-to-contact for each potential contact point was calculated by solving two linear equations for elevation versus time in-service. The first equation is for the contact point at the bottom of the CT and the second is contact point at the top of the LIN.

Figure 6 illustrates the process of calculating the CT-LIN time-to-contact, determined by the point of intersection of the CT and LIN elevations. In the figure, the elevation of the contact points on the CT and the LIN are plotted versus time in-service. The figure includes representations of the PLGS and Wolsong LIN elevation measurements and linear equations for the elevation of the contact points on the CT and the LIN.

Figure 6 – Illustration of the Process of Calculating CT-LIN Time-to-Contact

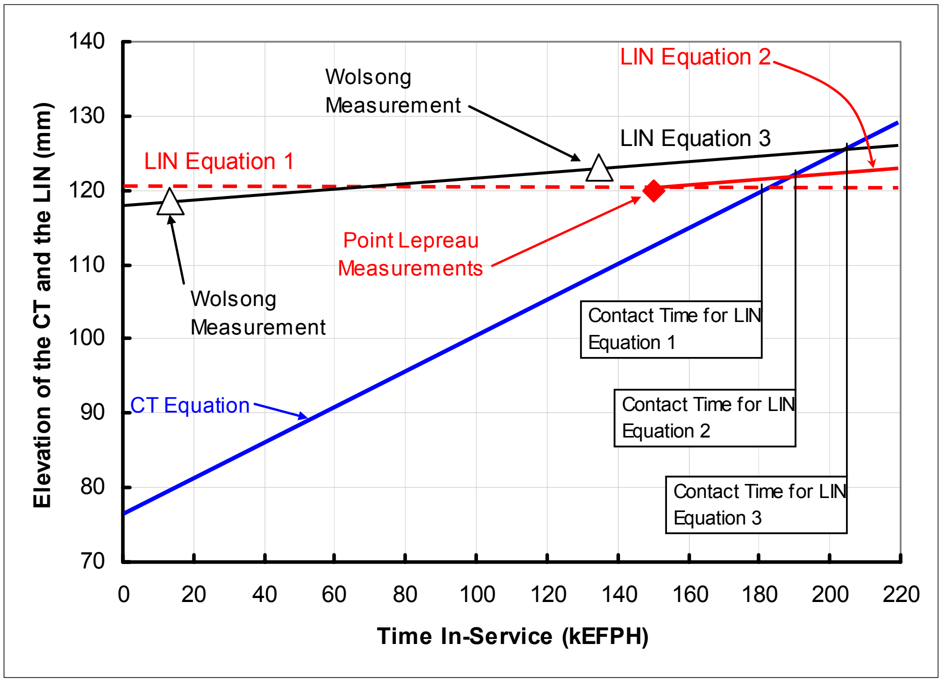

The elevation equation for the CT contact points was derived from CDEPTH 8.2 results with the updated model, described in Section 4.0.

As indicated in the figure, three different LIN elevation equations were derived. Equation 1 is based on LIN elevation measurements from PLGS, not crediting future sag of the LIN. Equation 2 is based on the same measurements but credits future creep sag of the LIN at an estimated rate. Equation 3 is based on Wolsong LIN elevation measurements that provided a linear equation for LIN elevation.

4.0 Updating of the CDEPTH fuel channel Models

In this paper the term, “updating” means the modification of input parameters in the standard CDEPTH fuel channel models to bring them up-to-date with recent developments, including calibration to measurements.

The standard CDEPTH fuel channel models were developed in the 1980s to predict the onset and spreading of CT-PT contact due to spacer movement. By necessity, high levels of conservatism were implemented in the standard models, as discussed in Sections 4.1 and 4.2.

4.1 Comparison of PT Sag Measurements and Predictions Using Standard CDEPTH Fuel Channel Models

For PLGS and Gentilly-2, it was found that predictions of PT sag using standard CDEPTH models overestimated recent in-service PT sag measurements. For example, Figure 7 shows the relationship between predicted PT sag and measured PT sag for PLGS. In the figure, M/P ratio (the ratio of Measured to Predicted sag) is plotted versus time in-service. A trend of decreasing M/P ratio with time in-service is indicated in Figure 7. For the 2004 inspection data, M/P ratio was found to range from 0.98 to 0.78.

Figure 7 – M/P Ratio for PT Sag Versus EFPH for the PLGS Pressure Tubes

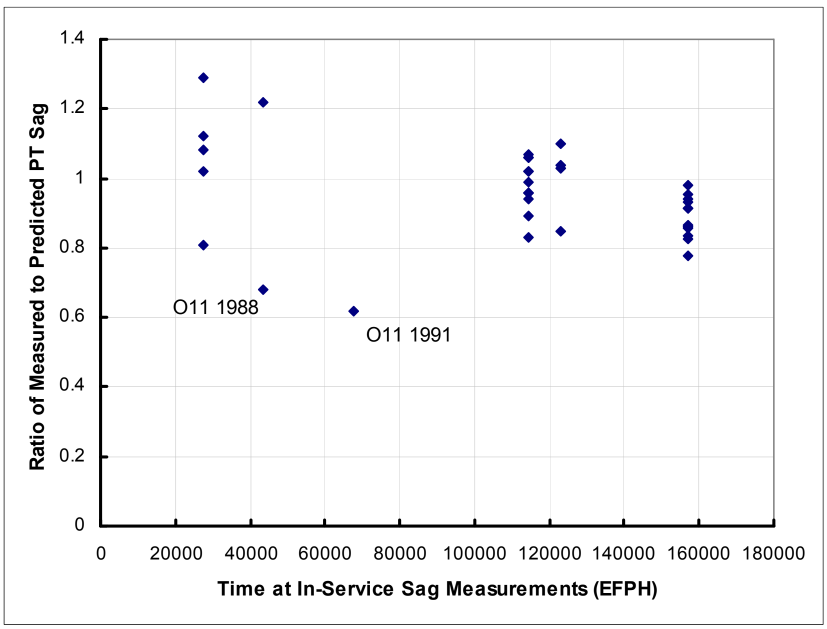

Note that the O11 measurements in 1988 and 1991 were investigated and discarded.

4.2 Measured Fuel Channel Spring-Back versus Spring Back Predicted with the Standard CDEPTH Model for F06

It was predicted, using the standard CDEPTH model for F06 that F06-L2 would spring back by 8.3 mm as a result of defuelling. The measured spring back at F06-L2 during the 2004 inspection was 4.5 mm.

4.3 Updates to the Standard CDEPTH Fuel Channel Model

The results presented in Sections 4.1 and 4.2 justified the modification of the standard CDEPTH fuel channel model for use in fuel channel sag predictions, in order to reduce the level of conservatism in the predictions of the model.

The following parameters in the model were investigated for potential modification:

1. PT In-Service Dimensions and CT End Bell Modelling
2. PT End Support Conditions
3. CT Ovality at Spacer Locations
4. The CT East End Support Condition

For Item 1, the PT in-service dimensions shown in Figure 2 were implemented in the CDEPTH model of the PT and the shape of the end bell was incorporated into the model of the CT for F06. For Item 2, the PT end point rotational degree of freedom was changed from free to fixed at both ends of the PT. For Item 3, the CT inner diameter profile of Figure 3 was incorporated into the CDEPTH model of the CT. For Item 4 the axial degree of freedom on the East end of the CT was changed from free to fixed.

The investigation of the CDEPTH modelling was carried out by successively introducing the above modifications to the standard CDEPTH model for F06 and executing four different models in CDEPTH to simulate the fuel channel spring back process for F06.

The models consisted of:

1. The standard model for F06
2. Modification 2 for F06 – Items 1 and 2, above
3. Modification 3 for F06 – Items 1, 2, and 3, above
4. Modification 4 for F06 – Items 1, 2, 3, and 4, above

The results of the spring back study are presented in Figure 8, in which spring back predictions for F06 are compared with the nominal measured spring back value. As shown, the standard model significantly over predicts the measured spring back value, indicating that the standard CDEPTH model for F06 is too flexible. With successive modifications to the model, increases in stiffness were realised but the measured spring back value was still over predicted using the Modification 4 model for F06.

Next, the effects of CT elastic modulus were studied. The study was conducted by executing the Modification 4 model for F06 in CDEPTH to predict spring back for various values of elastic modulus. A summary of the study is presented in Figure 9. The figure indicates that a doubling of the standard CT elastic modulus value would be required for the spring back prediction of the Modification 4 model to match the measured spring back value. At this point it is not known whether the actual elastic modulus of the CT in F06 could possibly be twice the standard value. Some associated information is provided in Section 5.0

As outlined in Section 2.9, the fuel channel fast neutron flux profiles in the standard CDEPTH models overestimate the actual flux to which the fuel channels were exposed. This suggested fast neutron flux as a parameter to be modified in updating the CDEPTH fuel channel models for PLGS.

Consequently, flux profiles for reduced power levels were generated for F06 and were incorporated into the updated CDEPTH model for F06 to simulate the derating of the reactor with time in-service. The updated model for F06, including the reduced flux profiles, was executed in CDEPTH 8.2 along with the standard model for F06. The results of the CDEPTH analyses for F06 are presented in Figure 10.

Two differences in the standard and updated models are apparent in Figure 10. First, the initial straight part of the sag deflection curve is lower for the updated model since its modifications provide a greater stiffness than the standard model. Second, starting at about 120 kEFPH, the reduced flux profiles in the updated model are manifested as a slight reduction in the slope of the CT sag curve for the updated fuel channel model.

Figure 8 – Predicted F06-L2 Spring Back Deflections from CDEPTH 8.2 Compared with Measurements

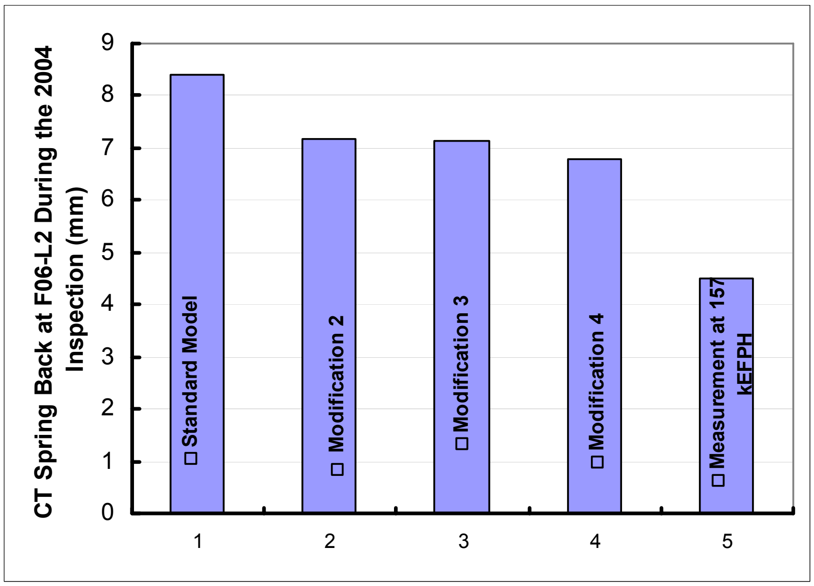

Figure 9 – F06 Spring Back Predictions with Modification 4 for Various Values of CT Elastic Modulus

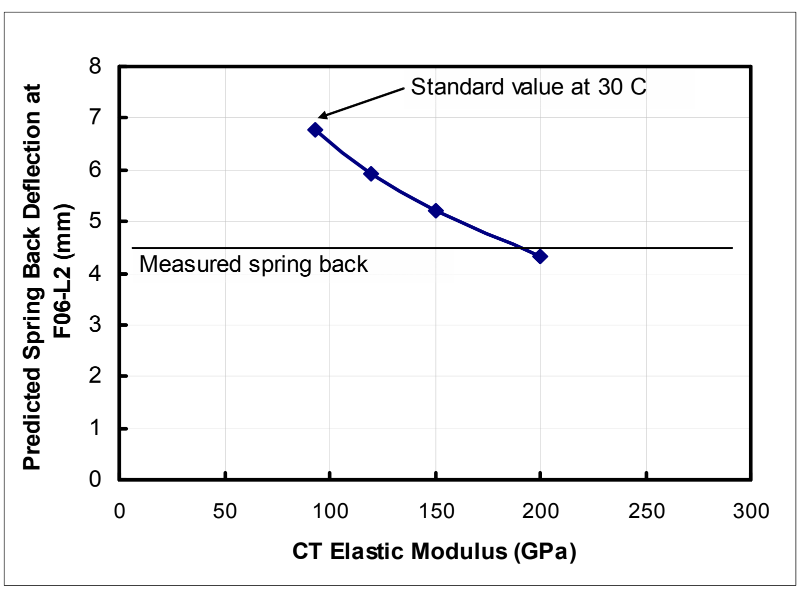

Figure 10 – Predicted CT Deflections for PLGS F06 Using Standard and Updated CDEPTH 8.2 Models

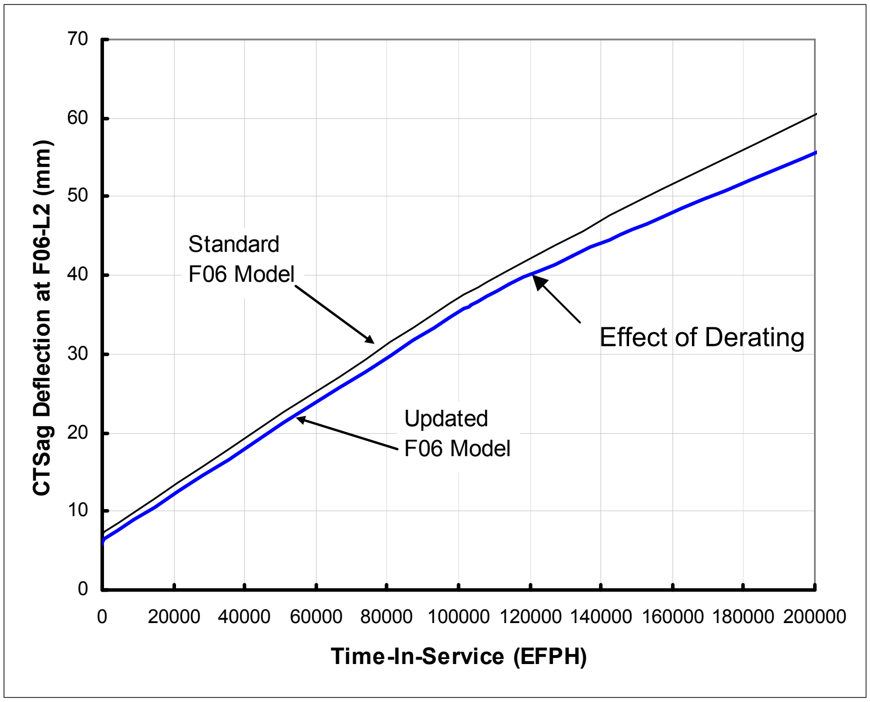

4.0 Predictions of CT Sag Using the Updated Fuel Channel Models

CT sag versus time in-service was predicted for the Row F and Row Q fuel channels in PLGS using the updated fuel channel models (Modification 4) with CDEPTH 8.2, including reduced flux profiles. Elevation versus time in-service values for the contact points on the CTs were extracted from the CDEPTH 8.2 outputs.

From CT elevation versus time in-service, linear equations for the elevations of the contact points on the CTs were derived. Table 4 presents a summary of the linear equations for the contact points on the CTs in Row Q.

Figure 11 provides a comparison of the CT creep sag rates for the standard and the updated CDEPTH models.

Table 4 - Parameter Values for the PLGS Row Q CT Elevation Equations

Contact Point	X_{CT} (m)	CT Sag Rate (mm/7k EFPH)	Intercept (mm)
Q02-L5	3.332	0.89	80.53
Q03-L5	2.903	1.26	82.52
Q04-L5	3.340	1.29	82.60
Q05-L5	2.898	1.42	82.27
Q06-L5	3.355	1.46	84.61
Q07-L5	2.899	1.67	82.11
Q08-L5	3.362	1.69	81.84
Q09-L5	2.903	1.62	82.41
Q10-L5	3.351	1.71	81.93
Q11-L5	2.902	1.75	79.91
Q12-L5	3.359	1.72	81.68
Q13-L5	2.899	1.71	81.15
Q14-L5	3.357	1.66	82.63
Q15-L5	2.903	1.71	81.21
Q16-L5	3.344	1.68	80.76
Q17-L5	2.901	1.60	83.38
Q18-L5	3.342	1.79	78.25
Q19-L5	2.899	1.33	83.75
Q20-L5	3.339	1.10	79.23
Q21-L5	2.905	1.09	77.65

X_{CT} is the distance from the outlet end fitting taper

Figure 11 – Comparison of Predicted Row Q CT Creep Sag Rates from Standard and Updated CDEPTH Fuel Channel Models for PLGS

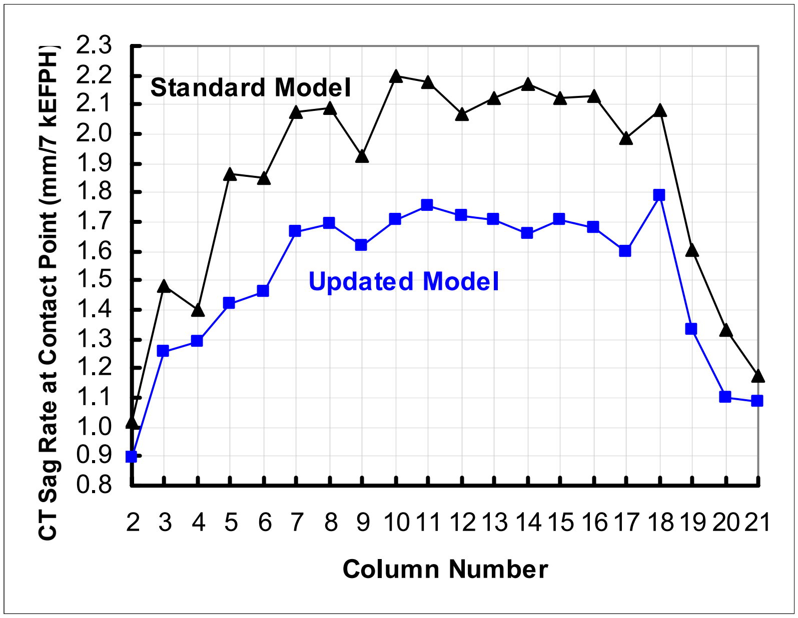

5.0 Use of In-Service PT Sag and CT-LIN Gap Measurements to Define the In-Service Elastic Curve of the LIN in PLGS

The in-service elastic curve of the LIN was determined in a three-step procedure:

1. The as-installed elevations of the support points of the LIN were found
2. The in-service elevations of the LIN were found at two axial locations where CT-LIN gaps were measured
3. Elastic curves were fitted through the support points and the two points with known elevations on the LIN for different end conditions at the pinned end of the LIN.

Although the LIN is pinned at the South end of the reactor, the actual support condition at that end is uncertain. Therefore, both fixed and pinned conditions were considered.

Accounting for as installed distances from the CT to the LIN, as-installed bow of the CTs, and as-installed sag of the CTs, the elevation of the LIN end points was determined to be 120.2 mm.

The in-service elevations of L5-Q07 and L5-Q08, were obtained as the sum of:

1. the measured sag of the PT (plus an adjustment for fuel weight effects)
2. the PT outer radius
3. the measured PT-CT gap
4. the CT wall thickness
5. the measured CT-LIN gap.

Table 5 provides the data used to calculate the elevations of LIN #5 and the results of the calculations

Table 5 – Measurements for Finding the Elevations of L5-Q07 and L5-Q08

Contact Point	PT Sag (mm) [1]	PT Outer Radius (mm)	PT-CT Gap (mm)[2]	CT-LIN Gap (mm)	CT Wall Thickness (mm)	LIN Elevation (mm)
L5-Q07	45.8	57.907	5.7	13.8	1.37	124.6
L5-Q08	46.6	57.168	5.3	14.2	1.37	124.9

Note 1: sag was measured with no fuel in the channel and was adjusted to account for the weight of the fuel and coolant under in-service conditions
Note 2: measured with no fuel in the pressure tube but with coolant and the inspection tool

Figure 12 illustrates the determination of the in-service elastic curves for LIN #5 from the support point elevations and the measurements at L5-Q07 and L5-Q08 for the two different end conditions at the pinned end of the LIN.

The elastic curve of the LIN from about 4500 mm to 7200 mm is practically independent of the South end support condition. For the rest of the LIN, the South end support condition has a small effect on the elastic curve.

For the PLGS assessment, it was not clear which LIN South end support condition should be used. It was subsequently decided that for the PLGS-specific assessment, a fixed support condition for the South end of the LIN would be assumed.

Figure 12 – Determination of the In-Service Elastic Curve for Lin #5 in PLGS at 157 kEFPH

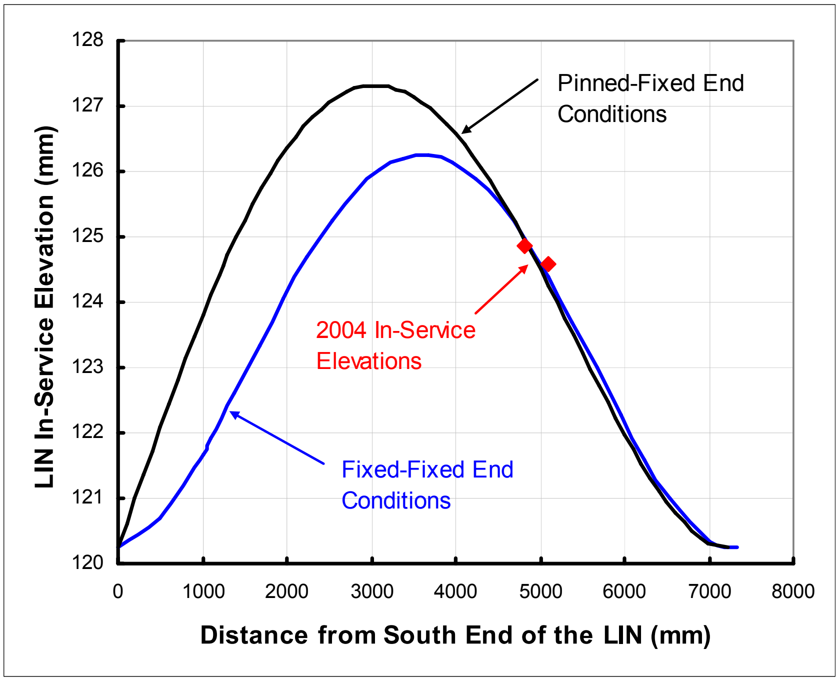

5.1 Evaluation of the In-Service Elastic Curve for LIN #5

From Figure 12, the maximum in-service sag of LIN #5 was determined to be 6 mm, whereas the initial sag of the LIN was predicted to be 14 mm [1]. A similar difficulty occurred in using the CDEPTH fuel channel model to predict spring back deflection, which will be discussed later. This inconsistency meant that the in-service measurements could not be combined with the predicted initial elastic curve to determine the rate of LIN creep sag, as planned for Reference [1].

Because of some discrepancies in the 2003 CT-LIN gap measurements for G-2, it was tentatively concluded that the method outlined in Section 5.0 tended to underestimate the elevation of the LIN in G-2, and by extension, in PLGS.

However, in the 2006 inspection of G-2, direct LIN sag measurements were obtained [8], from which an in-service elastic curve for LIN #5 in G-2 was produced. Figure 13 presents the in-service elastic curve and the four elevation measurements used to derive it.

Figure 13 – LIN #5 Elevation Measurements and Derived Elastic Curve for G-2 at 141.6 kEFPH

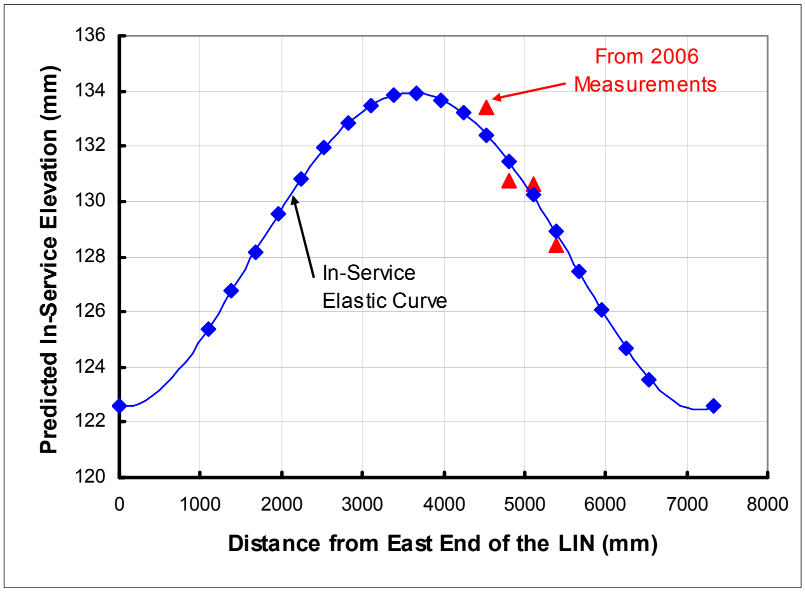

Comparing Figures 12 and 13, and in consideration of the Wolsong data presented in Section 7, the elevation of LIN #5 in Figure 12 is probably underestimated, which will lead to underestimations of the time-to-contact for PLGS.

Despite underestimating the actual sag of the LIN, the in-service LIN elevation of Figure 12 was used in the CT-LIN time-to-contact assessment for PLGS. The LIN elevation of Figure 12 was employed with the following assumptions: (1) that the LIN will not sag in the future, which is conservative, (2) that the LIN will sag at an estimated rate, derived in Section 6.

6.0 Estimation of the Creep Sag Rate for LIN #5

After the failure to deduce LIN creep sag rates from the inspection measurements, an estimated LIN creep sag rate was derived based on CRNL 4001, as follows.

Based on the ratio of bending stress and fast neutron flux for the LIN relative to Q12, the expected ratio of LIN/CT creep sag was calculated to be 0.20, assuming identical material properties. With a predicted creep sag rate of 1.51 mm/7 kEFPH for Q12, the creep sag rate of LIN #5 would be 0.303 mm/7kEFPH at the centre of the LIN.

7.0 Prediction of the Initial and In-Service Elastic Curves and LIN Creep Sag Rates from Inspections in Wolsong Units 1 and 4

Elastic curves for LIN #5 in Wolsong Unit 1 for fixed-fixed and pinned-fixed end conditions at 124.7 kEFPH were generated from the data in Table 2 of Section 2.7 and are plotted in Figure 14. Figure 14 shows that the end condition at the start of the LIN has a significant effect on the in-service elastic curve of the LIN. For time-to-contact to be conservatively under predicted, the magnitude of LIN in-service sag should be underestimated. Therefore, for the prediction of the in-service elastic curve, a pinned support condition was selected for the pinned end of the LIN.

Figure 14 – Determination of the In-Service Elastic Curve for LIN #5 In Wolsong Unit 1 at 126.7 kEFPH

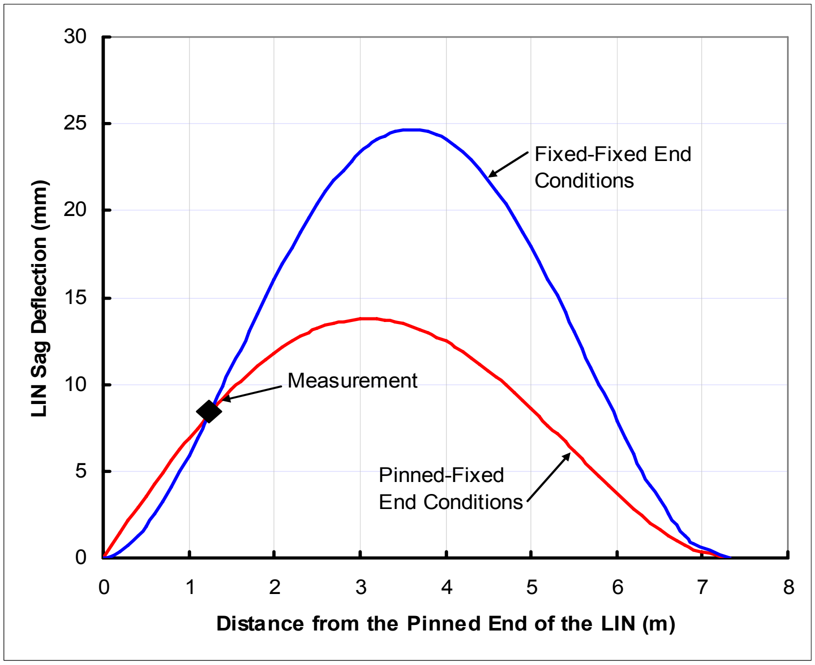

Next, the initial elastic curve of the LIN for Wolsong was determined from the LIN sag measurements, as illustrated in Figure 15.

Using the initial and in-service elastic curves in Figure 15, LIN creep sag rates were calculated and are presented in Figure 16. Figure 16 also includes a plot of the estimated LIN creep sag rates for PLGS from Section 6.0, for comparison.

Figure 15 – In-Service and Derived Initial Elastic Curve for LIN #5 in Wolsong

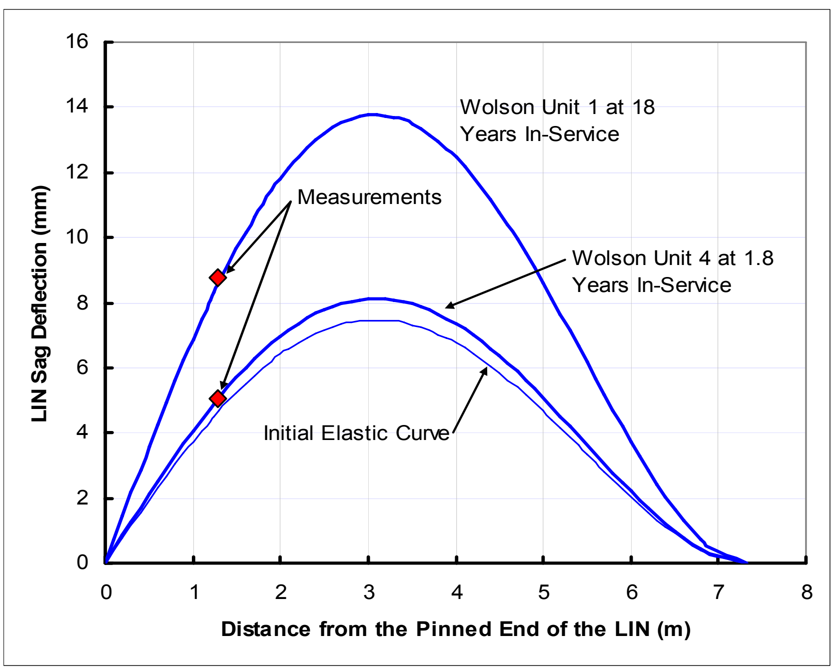

Figure 16- Creep Sag Rates for Wolsong LIN #5 and Estimated Creep Sag Rate for PLGS LIN #5

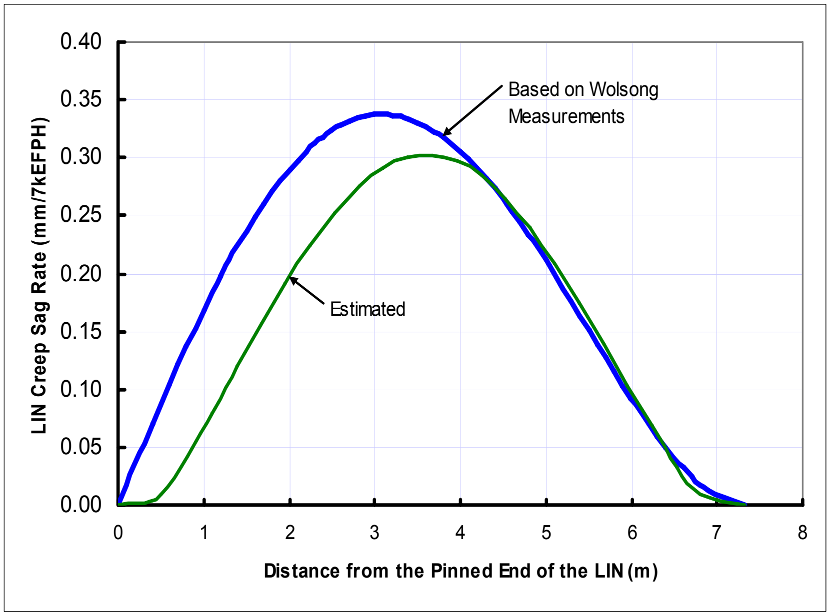

7.1 Comparson of LIN Elastic Curves Based on Wolsong Measurements and the 2006 LIN Sag Measurements for G-2

Figure 17 presents the predicted in-service sag at 141 kEFPH for LIN #5 from the Wolsong measurements for comparison with the 2006 LIN sag measurements at G-2. The sag profile for two different end support conditions are shown for the G-2 LIN. Figure 17 shows that the Wolsong and the 2006 G-2 LIN sag measurements produce similar LIN sag profiles provided that pinned-fixed end conditions are assumed for the LIN.

Figure 17 - Predicted Elastic Curves at 141.5 kEFPH For LIN #5 in Wolsong and G-2

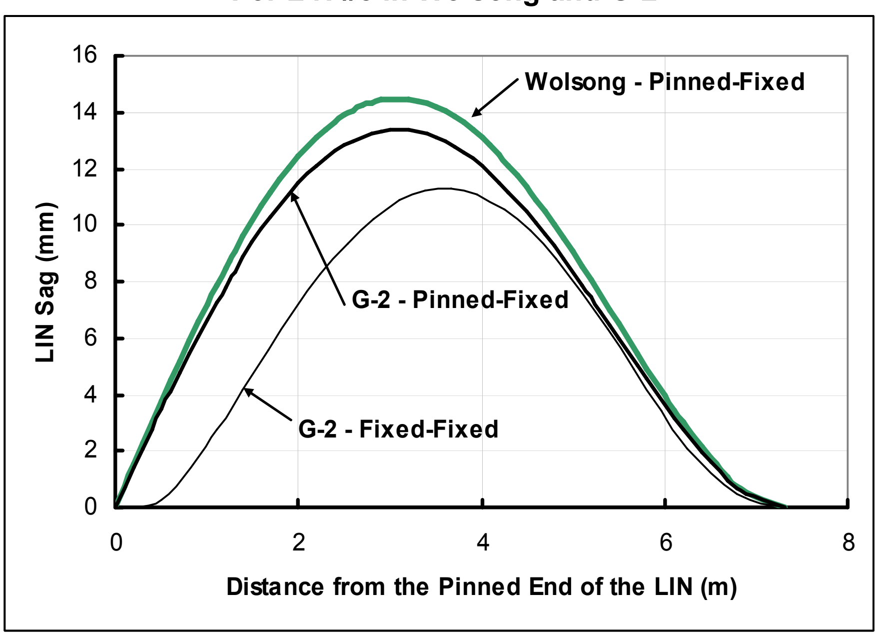

8.0 Predictions of CT-LIN Time-to-Contact for PLGS and Gentilly-2

Time-to-contact predictions for PLGS and G-2, using reactor-specific LIN elevation measurements are presented in Sections 8.1 and 8.2. Section 8.3 provides predictions for G-2 based on the use of Wolsong LIN creep sag properties. Section 8.4 presents an alternative treatment for predicting CT creep sag rates to validate the updated fuel channel models.

8.1 Predictions for PLGS Using Reactor-Specific LIN Elevation Measurements

Time-to-contact predictions for PLGS were performed using the CT elevation equations of Table 4 and the LIN elevations of Figure 12, assuming two different LIN sag rates: (1) zero creep sag beyond that at the 2004 inspection, and (2) creep sag at the estimated rate from Section 6.0. Figure 18 presents a summary of the time-to-contact analysis.

As shown in Figure 18, it was predicted that none of the channels in Row Q would be subject to CT-LIN contact by 185 kEFPH. For no future creep sag of the LIN, it is predicted that CT-LIN contact would first occur in Q06 at 206 kEFPH.

Figure 18 – Time-to-Contact Predictions for the PLGS Row Q Fuel Channels Using Updated Fuel Channel Models With Different LIN Creep Sag Rates

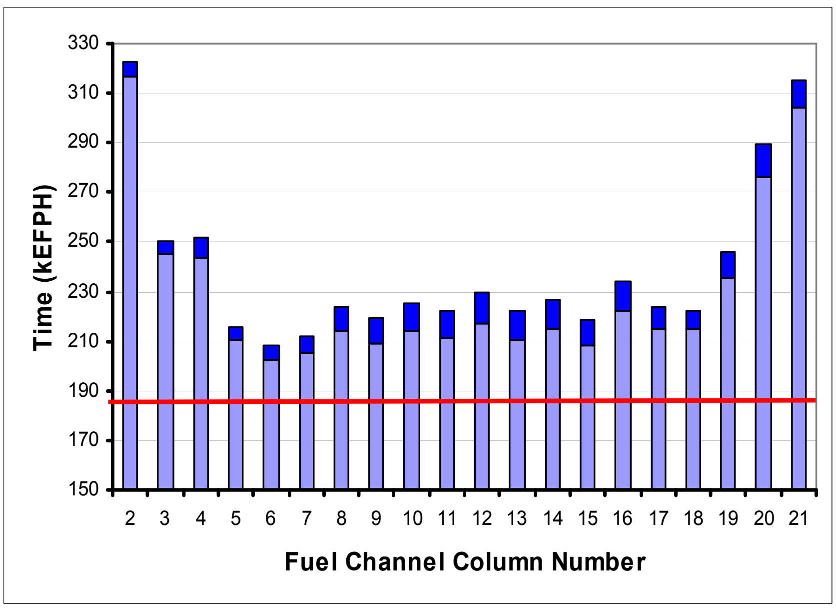

Note: the light bars represent time-to-contact for zero creep sag of the LIN beyond 157 kEFPH. The dark bars represent the increase in time-to-contact for creep sag of the LIN at the estimated rate. The total height of the light and dark bars represents the time-to-contact for creep sag of the LIN at the estimated rate. The horizontal line represents the planned time in-service for plant shutdown for retubing.

8.2 Predictions for Gentilly-2 Using Reactor-Specific LIN Elevation Measurements

The analysis of Section 8.1 was repeated for G-2 using reactor-specific CT and LIN elevation equations described in Sections 8.2.1 and 8.2.2. For this assessment it was assumed that G-2 will by shut down for retube at 196 kEFPH.

8.2.1 CT Elevation Equations for G-2

Table 6 [4] provides elevation equations for the contact points on the Row Q CTs in G-2, obtained from the predictions of the updated G-2 fuel channel models.

Table 6 - Parameter Values for the G-2 Row Q CT Elevation Equations

Contact Point	X_{CT} (m)	CT Sag Rate (mm/7 kEFPH)	Intercept (mm)
Q02-L5	3.319	0.77	123.52
Q03-L5	2.898	0.98	124.70
Q04-L5	3.330	1.50	126.05
Q05-L5	2.895	1.39	127.48
Q06-L5	3.330	1.44	128.89
Q07-L5	2.898	1.50	130.23
Q08-L5	3.337	1.36	131.42
Q09-L5	2.900	1.51	132.42
Q10-L5	3.338	1.57	133.19
Q11-L5	2.902	1.51	133.69
Q12-L5	3.340	1.51	133.91
Q13-L5	2.900	1.53	133.83
Q14-L5	3.345	1.51	133.47
Q15-L5	2.900	1.55	132.83
Q16-L5	3.343	1.46	131.95
Q17-L5	2.900	1.47	130.84
Q18-L5	3.334	1.48	129.57
Q19-L5	2.892	1.22	128.18
Q20-L5	3.324	0.98	126.75
Q21-L5	2.900	0.79	125.35

X_{CT} is the distance from the outlet end fitting taper

8.2.2 LIN #5 Elevation Equations

CT elevation equations for LIN #5 were derived based on Figure 13, assuming two different LIN sag rates: (1) zero future creep sag of the LIN (beyond that at the time of the 2006 inspection) and (2) creep sag of the LIN at the estimated rate from Section 6.0.
.

8.2.3 CT-LIN Time-to-Contact Predictions

The results of the CT-LIN time-to-contact analysis for G-2 are presented in Figure 19. As indicated in Figure 19, it was predicted that none of the Row Q CTs in G-2 will contact LIN #5 at 196 kEFPH. It was predicted that the earliest contact would occur in Q04 at 235 kEFPH, conservatively assuming no further creep sag of the LIN beyond 141.6 kEFPH.

Figure 19 - Time-to-Contact Predictions for the G-2 Row Q Fuel Channels Using Updated Fuel Channel Models With Different LIN Creep Sag Rates

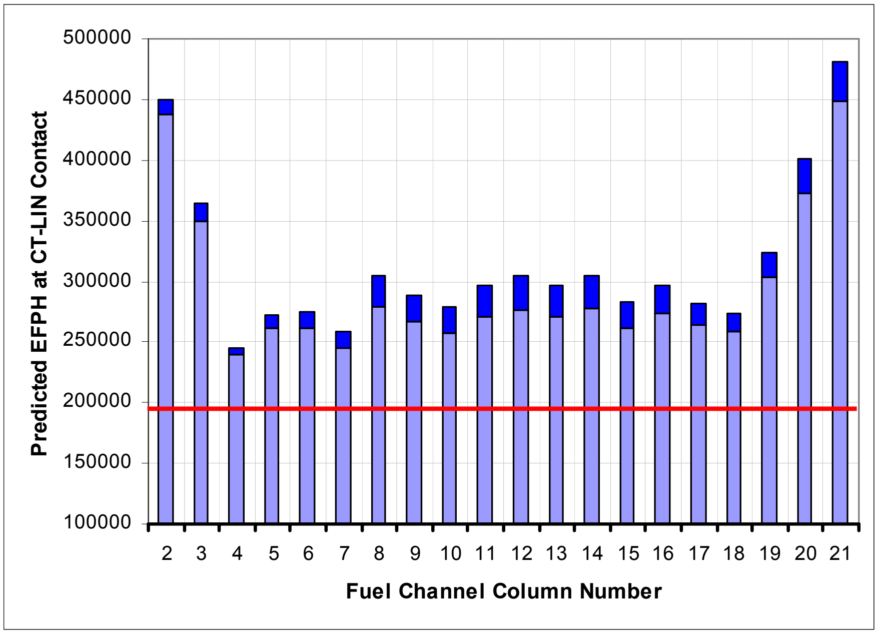

The notes to Figure 18 apply here,

8.3 Assessment for Gentilly-2 Using Wolsong LIN Elevation Data

The purpose of this analysis is to investigate the use of the Wolsong LIN elevation equations to predict CT-LIN contact in G-2. The CT elevation equations used in this analysis are the same as those given in Section 8.2.1.

8.3.1 LIN #5 Elevation Equations

For this analysis the intercepts for the LIN elevation equations were obtained from the initial elastic curve of Figure 15. The LIN creep sag rates given in Figure 16 were used to determine the slopes for the LIN elevation equations.

8.3.2 CT-LIN Time-to-Contact Predictions

Time-to-contact predictions for the Row Q fuel channels in G-2, using the creep sag properties of LIN #5 in Wolsong, are presented in Figure 20. Comparing Figures 19 and 20, there is a general improvement in the time-to-contact with the use of Wolsong LIN elevation measurements instead of the G-2 LIN elevation measurements. With the Wolsong LIN creep sag properties, Q04 is still the critical channel with contact predicted at 250 kEFPH, rather than at 235 kEFPH, with G-2-specific LIN elevation measurements.

Figure 20 – Time-to-Contact Predictions for the G-2 Row Q Fuel Channels Using Updated Fuel Channel Models With Wolsong LIN Creep Sag Rates

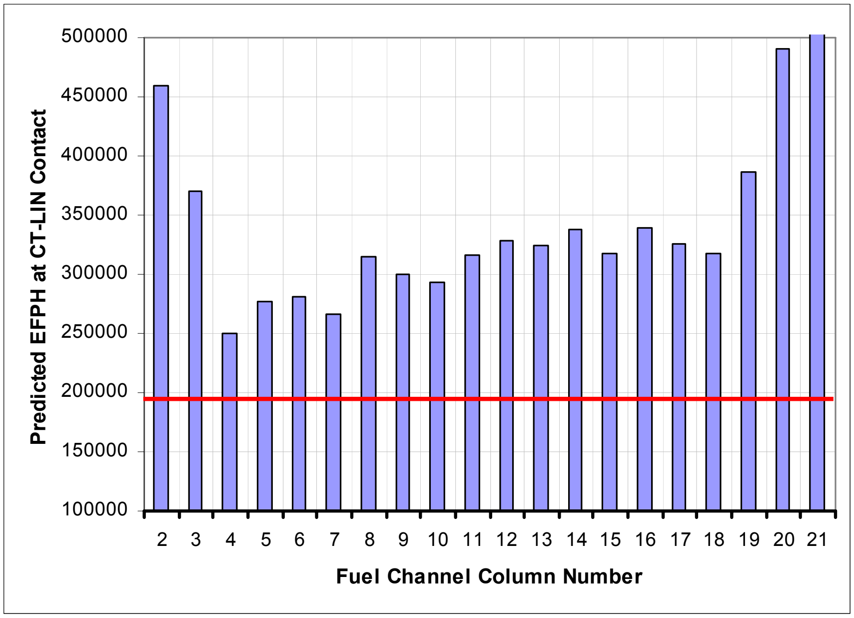

The notes to Figure 18 apply here,

9.0 Discussion of Results

9.1 LIN Creep Sag Behaviour

Under predictions of LIN elevation from the G-2 CT-LIN gap measurements and indications from Figure 12 for PLGS show that the method of combining PT sag measurements with CT-LIN gaps underestimates the sag of the LIN.

However, direct measurements of LIN sag, performed in G-2 and in Wolsong Units 1 and 4 have produced reasonable in-service elastic curves and creep sag rates for LIN #5. It is important to note that the LIN #5 sag rate from the Wolsong measurements matches the estimated LIN sag rate for G-2 and that the in-service elastic curve at 141.6 kEFPH for G-2 agrees well with that for Wolsong. The creep sag behaviour of the Wolsong LIN has therefore been confirmed by an alternative method.

9.2 CT Creep Sag Rate Predictions

To illustrate the level of conservatism in the updated fuel channel models, predicted and measured CT elevation values for Q06 at 141.6 kEFPH are compared in Figure 21. Q06 is a typical channel. Figure 21 indicates that there is still some conservatism in the updated fuel channel model.

Figure 21 – Comparison of Predicted CT Elevation vs Time In-Service with CT Elevation from PT Sag Measurements for Q06-L5

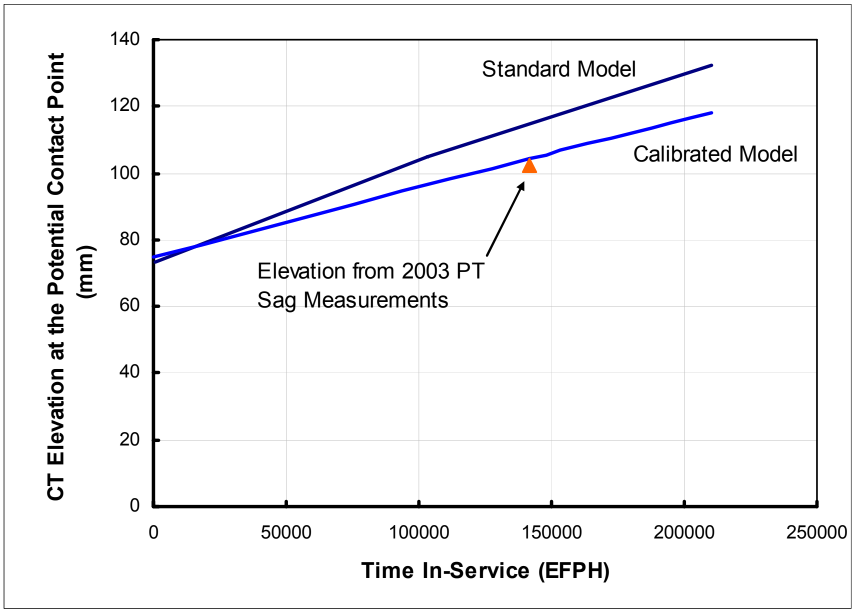

9.2.1 Alternative Treatment for CT Creep Sag Rate Predictions

The treatment of CT creep sag rate up to this point has been purely analytical. It would be beneficial to validate the CT creep sag rate predictions through the use of an alternative method. For this purpose the PT sag data was used in a statistically-based treatment, as follows.

Figure 22 is a plot of measured PT sag versus channel power for the Row Q in G-2. All the data points in the figure were measured at 141.6 kEFPH. The regression line and 95% upper prediction limit for PT sag versus channel power are plotted in the figure.

Figure 22 – Measured PT Sag for Row Q Channels in G-2 Vs Channel Power

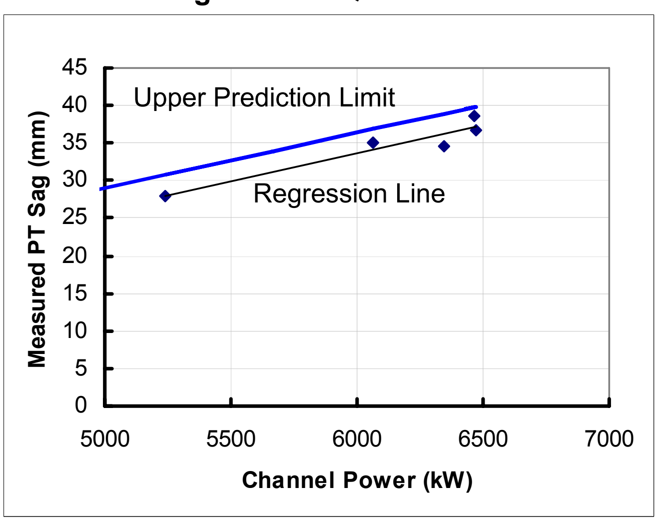

The upper prediction limit for PT sag vs channel power was used to predict PT sag for the Row Q channels at 141.6 kEFPH as depicted in Figure 23. Measured PT sag values are also plotted in Figure 22 for comparison with the predicted upper bound values.

Figure 23 – Predicted Upper Bound PT Sag for the Row Q Channels in G-2 at 141.6 kEFPH

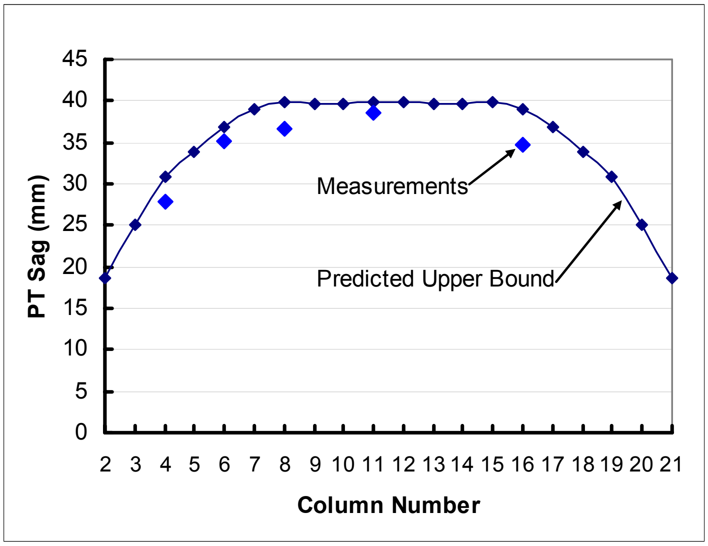

Next, PT sag versus time curves were fitted through each of the predicted upper bound PT sag values for the Row Q channels of the form:

$$Sag = a\, t^b$$

where a and b are constants and t is the time in-service.

The power function fit to PT sag versus time in-service was determined by trial and error using STATGRAPHICS 5.1, and is plotted in Figure 24.

Figure 24 – PT Sag Measurements in G-2 versus Time In-Service

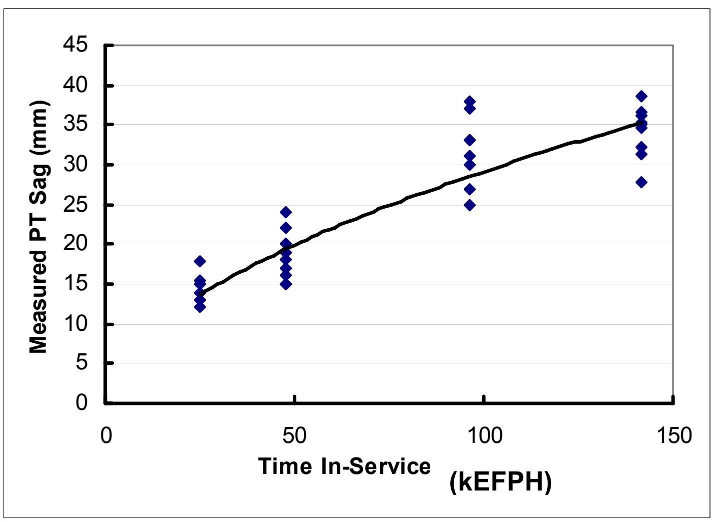

Finally, the PT sag versus time functions for the channels were differentiated with respect to time to generate CT creep sag rates for the Row Q channels in G-2, given in

Figure 25. Comparing Figures 11 and 25, it is seen that the alternative treatment of CT creep sag rate presented above predicts somewhat lower CT creep sag rates than those derived from the updated fuel channel models. Although conservatism was removed in the process of updating the fuel channel models, an amount still remains. This is partially because the CT elevation equations are linear with time in-service whereas in the alternative treatment, a non-linear trend for CT elevation vs time was employed.

Figure 25 – Predicted Upper Bound CT Creep Sag Rates for the G-2 Row Q Fuel Channels

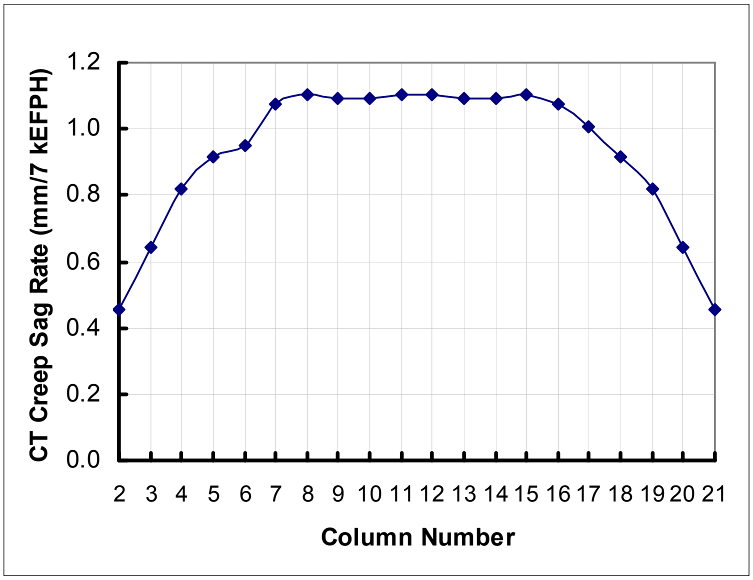

It is interesting that both the LIN and fuel channel structural models under predict the stiffness of the actual components relative to measurements. This observation points to the possible need to adjust elastic modulus values in the structural models.

10.0 Conclusions

1. The standard CDEPTH fuel channel models for PLGS and G-2 underestimate fuel channel stiffness and overestimate PT in-service sag, compared with measurements, resulting in under predictions of the time-to-CT-LIN contact.

2. The following details in the standard CDEPTH fuel channel models contribute to over predictions of PT sag: (1) free rotational degrees of freedom on the ends of the PT, (2) a free axial degree of freedom on the East end of the CT, (3) the use of PT flux profiles based on time-averaged reactor power levels compiled for 1993. With updates to these modelling details, the CT in-service sag predictions closely match CT sag values based on PT sag measurements.

3. The Wolsong LIN sag measurements currently provide the best estimate of LIN creep sag behaviour for use in CT-LIN time-to-contact predictions for CANDU 6.

4. Based on the results in Figures 18 and 19, it is concluded that CT-LIN contact could not have occurred in PLGS by 185 kEFPH and will not occur in G-2 by 196 kEFPH.

11.0 References

1. P.J. Sedran, CPUS Limited, *Scoping Analysis for the Prediction of Onset Times for CT-LIN Contact in PLGS*, 0028-REPT-ENG-001 Rev. 01, August 2, 2005.

2. P.J. Sedran, CPUS Limited, *CT-LIN Time-to-Contact Predictions for PLGS using Updated FC Models*, CPUS Technical Report 0040 REPT ENG 0003 00, September 30, 2005.

3. P.J. Sedran, CPUS Limited, *Update to Time-to-Contact Predictions for CT-LIN Contact in PLGS using Calibrated Fuel Channel Models*, CPUS Technical Report 0065 REPT ENG 0005 00, October 30, 2007.

4. P.J. Sedran, CPUS Limited, *Prediction of Onset Times for CT-LIN Contact in Gentilly-2*, CPUS Technical Report 0078 REPT ENG 0001 00, October 15, 2007.

5. T.R. Kim, S.M. Sohn, J.S. Lee, Korea Electric Power Research Institute, *Ultrasonic Devise to Measure Gap Between Calandria Tube and LISS Nozzle*, 7th International CANDU Maintenance Conference, Toronto, November 20 – 22, 2005.

6. W. Mayo, *Fuel Channel Periodic Inspection: 2004, May, Final Report*, AECL Report 87-31100-PIP-003, January, 2005.

7. T. Campbell, *AECL Inspection Report Calandria Tube to LISS Nozzle Gap Measurement*, 87-31230-INR-001 Revision 1, January 2005.

8. D. Kalenchuk, AECL, *Inspection Report Calandria Tube to LISS Nozzle Gap Measurement Gentilly-2,* 66-31230-INR-002, Revision 1D1, to be issued.

12.0 Acknowledgments

Trevor Langlais, John Slade, and Ray Baker of NB Power Nuclear, and Philippe Charest and Luc Pedneault of Hydro-Québec contributed to this work.